Modeling of the cardiac sympathetic nervous system and the contribution of epicardium-derived cells

Ge, Y.

3

THE SEX OF EPICARDIUM-DERIVED CELLS INFLUENCES THE OUTGROWTH OF CARDIAC SYMPATHETIC NERVES IN VITRO

Yang Ge[1,2], Janine M. van Gils[5*], Ruben Methorst[1*], J. Conny van Munsteren[1], Anke M. Smits[3], Marie-José T.H. Goumans[3], Thomas J. van Brakel[4], Martin J. Schalij[2], Marco C. DeRuiter[1#], Monique RM. Jongbloed[1,2#]

* Shared authorship

Shared senior authorship

1. Department of Anatomy & Embryology, Leiden University Medical Center, Einthovenweg 20, 2333 ZC Leiden, The Netherlands;
2. Department of Cardiology, Leiden University Medical Center, Albinusdreef 2, 2333 ZC Leiden, The Netherlands;
3. Department of Cell and Chemical Biology, Leiden University Medical Center, Einthovenweg 20, 2333 ZC Leiden, The Netherlands;
4. Department of Thoracic Surgery, Leiden University Medical Center, Albinusdreef 2, 2333 ZC Leiden, The Netherlands;
5. Department of Nephrology, Leiden University Medical Center, Albinusdreef 2, 2333 ZC Leiden, The Netherlands;

Ready for submission

ABSTRACT

In the past decades, attention on sex differences in the prevalence and outcomes of a wide range of cardiac diseases has increased. Next to overt sex differences in disease presentation and outcome, also differences in autonomic function between males and females have been exposed. After myocardial infarction (MI), male patients have an increased risk for ventricular arrhythmias and sudden cardiac death. Part of these arrhythmias have been attributed to an increase in cardiac sympathetic nerve fibers occurring after cardiac damage. Although mechanical studies of post-MI cardiac sympathetic hyperinnervation have raised growing awareness on the role of the autonomic nervous system in arrhythmogenesis, data on the role of sex herein are still scarce and not conclusive. Here we show that male co-cultures of superior cervical ganglia with male myocardium and mesenchymal epicardium-derived cells (EPDCs) resulted in significant higher neurite directional outgrowth towards myocardium compared to entirely female co-cultures. Moreover, male EPDCs in a female setting enhanced the female neurite outgrowth comparable to an entire male environment. RNA sequencing of male and female EPDCs revealed that female EPDCs have a higher expression of the axon-repellent guidance cue SLIT2, which was also confirmed at the protein level. Our results confirm the stimulating effect of EPDCs on neurite outgrowth and also demonstrate that sympathetic nerve outgrowth and density differs between male and female in vitro which can be equalized by changing the sex of the EPDCs. Our data underlines the potential relevance of sex differences in post-MI cardiac hyperinnervation.

Keywords

Sex differences, sympathetic hyperinnervation, epicardium-derived cells, superior cervical ganglion, ventricular myocardium

INTRODUCTION

Cardiovascular disease is the most important cause of death in Western countries. Sudden cardiac death is a worldwide public health challenge, and is commonly associated with ischemic heart disease [1, 2]. In the past decades, attention on the influence of sex in the prevalence and outcomes of a wide range of cardiac diseases has increased. Next to overt sex differences in cardiovascular disease presentation and outcome [3, 4], also differences in autonomic function between males and females have been exposed [5-7]. Although ischemic cardiovascular disease occurs more often and seems prone to an adverse outcome in males, females seem to obtain a similar risk at cardiovascular events at higher age [3, 8-10]. Partly, this has been attributed to changes in hormonal status, related to menopause, hypothesizing that the lack of estrogens provide a more "male environment" with a concomitant higher cardiovascular risk profile [11].

After myocardial infarction (MI), patients are at increased risk for ventricular arrhythmias and sudden cardiac death. Part of these arrhythmias have been attributed to the phenomenon of cardiac sympathetic hyperinnervation, an increase in sympathetic nerve fibers in the heart which occurs after cardiac damage [12-14]. Several studies have reported sex related differential gene expression in sympathetic genes, as well as differential neurotransmitter contents in rodent studies [15, 16]. Although mechanical studies of post-MI sympathetic hyperinnervation have raised growing awareness on the role of the autonomic nervous system in arrhythmogenesis, data on the role of sex herein is still deficient.

Previously we have reported a stimulating effect of activated mesenchymal epicardium-derived cells (EPDCs) on neurite outgrowth of sympathetic ganglia [17]. The outer layer of the heart, or epicardium, is composed of multifunctional and multipotential progenitor cells with important roles during heart development [18, 19]. In the healthy adult heart these cells are quiescent, but they can become activated in response to pathological triggers, such as MI [18, 19]. Epicardial cells then migrate into the subepicardial space and myocardium, whereafter they are referred to as EPDCs. These cells can differentiate into a.o. coronary smooth muscle cells and cardiac fibroblasts [19, 20]. In our previous study, we showed increased directional outgrowth of sympathetic ganglia towards myocardium in vitro in the presence of human mesenchymal EPDCs [17]. No sex comparison was included as the sex of the used human EPDCs obtained from surgical procedures was unknown to us. To explore whether the stimulating role of EPDC in neurite outgrowth is sex dependent we designed new co-culture experiments including the biological sex origin. RNA sequencing of both male and female EPDCs were performed to find first clues in found differences between male and female hyperinnervation.

MATERIALS AND METHODS

Experimental animals and tissue isolation

C57BL/6J (Charles River) adult mice (n = 30) and mice embryos of embryonic day (E) 18.5 (n = 119) were used. All animal experiments were carried out according to the Guide for the Care and Use of Laboratory Animals published by NIH and approved by the Animal Ethics Committee of the Leiden University (License number AVD1160020185325, Leiden, The Netherlands).

For the dissection and pre-culture of adult murine myocardium, female mice and male mice were euthanized in a CO_2 chamber. Left ventricular myocardium was isolated and cut into pieces of 0.1mm^3. The myocardium pieces were cultured in EPDC medium (at 37 °C and 5% CO_2) for 7 days before subsequent co-culturing. EPDC medium is a 1:1 mixture of low glucose Dulbecco's modified Eagle's medium (10567014; Thermo Fisher Scientific) and medium 199 (31150022; Thermo Fisher Scientific) with 10% heat-inactivated fetal bovine serum (FBS; S1860-500; Biowest) and 1% 100× penicillin/streptomycin solution (15140122; Thermo Fisher Scientific).

For the isolation of murine embryonic superior cervical ganglia, pregnant mice were euthanized with CO_2, whereafter E18.5 embryos were collected and euthanized in cold PBS. The sex of embryos were determined based on the internal genitalia and confirmed by PCR. To isolate superior cervical ganglia (SCG), the embryonic skin was opened along the midline of the neck to expose the bilateral bifurcations of the common carotid arteries. Cervical ganglia were first dissected together with carotid arteries and placed in cold PBS. Thereafter, vascular and connective tissues were removed from SCG under a stereomicroscope. Each SCG was processed into 4 pieces for subsequent co-culturing and kept in cold PBS for further application.

Isolation and culture of human EPDCs

Adult human atrial samples (auricles) were collected as surgical waste material, and further processed anonymously with only the sex of the donor known. Handling of human heart tissues was carried out according to the Dutch regulation for responsible use of human tissues for medical research purposes, and the institutional Medical Ethics Committee ruled that the Medical Research Involving Human Subject Act (WMO) does not apply to the use of surgical waste material (reference number B12.017). EPDCs were isolated from the auricles and EMT was induced to obtain mesenchymal EPDCs, as previously described [21]. Briefly, the epicardium was carefully removed from the underlying myocardium and cut into small pieces followed by three incubations in 0.25% Trypsin-EDTA (25200056; Thermo Fisher Scientific) at

37 °C for 30 min in total. After digestion, the cell suspension was passed through a series of syringes of decreasing internal diameter (19G to 22G) and through a 100-µm BD Falcon cell strainer (BD Biosciences). Next, the cells were plated on 0.1% porcine gelatin coated dishes (G1890; Sigma-Aldrich) and cultured in EPDC medium. To ensure that the cells were derived from the epicardium, only cultures that displayed a clear epithelial morphology were used for further experiments. Mesenchymal EPDCs were obtained after five days of TGFβ (1 ng/ml) stimulation, cultured for a few passages in a mesenchymal state and cryo-preserved in freezing medium (10% DMSO, 25% FBS and 65% EPDC medium) in liquid nitrogen until further use. Cryo-preserved human mesenchymal EPDCs were thawed and cultured for a week before use in the co-cultures.

Co-cultures and neurite outgrowth assay

As indicated in **Figure 1A**, ventricular myocardium explants and cryo-preserved male and female EPDC aggregates were prepared 4 days prior to co-culturing with SCG in a 3D collagen gel in vitro. EPDCs of passage 6 to 9 were collected and split into sterilized microtubes at a density of 10^4 cells per tube. After centrifugation at 1,000 rpm for 4 minutes, the supernatant was carefully removed and 4 µl collagen gel mix was added in each tube without mixing. Microtubes were incubated for 10 minutes in a cell incubator followed by the addition of 80 µl complete medium in each tube. To make gel mix, 1.5 ml type I collagen gel (Corning 35429), 500 µl 10X PBS and 34.5 µl 1N NaOH were added into 3 ml culture medium and kept on ice. To perform co-culturing, 50 µl of collagen gel mix was placed in the center of 24-well plates and allowed to solidify at 37°C. Once collagen gel was solidified after 20 minutes, cervical ganglion pieces with or without other co-culture cells/tissue were transferred onto the solidified gel drops and another 50 µl collagen gel mix was added to encapsulate the tissue explants. The plate was kept in the incubator for 20 minutes before 500 µl complete culture medium was added. According to the cell/tissue components employed in the (co-)culture condition, a total of 4 conditions were included in the study (**Fig. 1B**): *control condition* (only SCG explants); *EPDCs condition* (SCG co-culturing with EPDCs); *M condition* (SCG co-culturing with pre-cultured myocardium) and *M+EPDCs condition* (SCG co-culturing with both pre-cultured myocardium and EPDCs). All the co-cultures were allowed to sprout for 6 days, after which the cultures were fixed and neurite outgrowth was quantified.

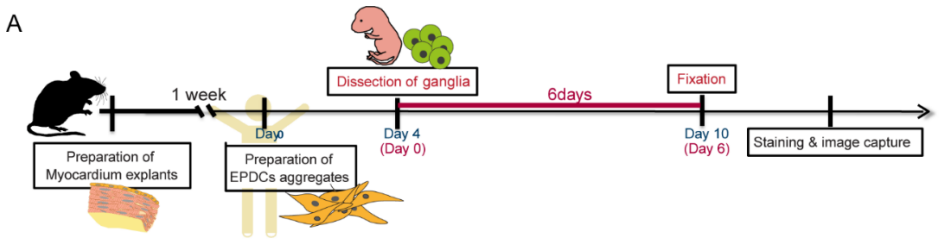

B

Control	+	-	-
EPDCs condition	+	+	-
M condition	+	-	+
M+EPDCs condition	+	+	+

Figure. 1 Experimental workflow and co-culture conditions. A. Schematic timeline of events in co-culturing superior cervical ganglia (SCG) with solely mesenchymal EPDCs or with mesenchymal EPDCs in co-culture of left ventricular myocardium. B. Schematic illustration of co-culture conditions.

Quantification of neurite outgrowth

After 6-day culture, the medium in the culture plates was removed followed by rinsing with PBS and fixed with 4% PFA for 30 minutes at room temperature (RT). Next, the samples were permeabilized with 0.5% Tween 20 for 30 minutes and blocked with 1% BSA in PBS with 0.05% Tween 20 for 1 hour at RT. The samples were incubated with primary antibody rabbit anti β-Tubulin III (anti-Tubb3) (Sigma T2200; 1:500) (a general staining for autonomic nerve fibers) overnight at 4°C. After 3 rinses with PBS, the samples were incubated with Alexa Fluor-488 donkey anti-rabbit IgG(H+L) (Life Technology A-21206; 1:250) for 2.5 hours. DAPI was stained after secondary antibody incubation to indicate nuclei. Images of ganglia were captured with a Leica AF6000 microscope.

To quantify "*directional neurite outgrowth*" (i.e. outgrowth towards the myocardium), first all outgrowth results were classified into 3 groups (no outgrowth, non-directional outgrowth and directional outgrowth) according to the presence of neurite outgrowth and its directional preference as was illustrated previously [17]. In short, once directional outgrowth was detected, anti-Tubb3 images were processed by the Image J Quadrant picking plug-in (ImageJ version 1.52p, National Institutes of Health, Bethesda, MD), which divided the image in 4 quadrants according to the ganglion-myocardium position. The quadrant facing the myocardium/EPDC aggregate was selected, and the neurites sprouting towards the myocardium/EPDC aggregate in the selected quadrant were quantified using the NeuriteJ

plug-in, as described by Torres-Espin et al. [22]. Briefly, SCG explants were identified and circles (with an interval of 25 µm) surrounding SCG were produced automatically in NeuriteJ. The number of directional neurites was automatically calculated by counting cross points of neurites and circles.

To correct for potential differences in the amount of myocardium used in each experiment, all data were normalized for myocardial volume. The volume of each myocardial sample used in each co-culture was measured with a confocal microscope (Leica SP8 or Dragonfly 200) by detecting autofluorescence of myocardium. Z-stack (10um per step) and tile scan options of confocal microscopy were applied during imaging.

$$Volume\ of\ myocardium\ =\ stacked\ area\ of\ all\ stacks\ \times thickness\ per\ step$$

The myocardium volume of the myocardium used in the first co-culture was considered as reference volume, and the volumes of the rest of the myocardium was calculated relative to this reference volume.

The normalized directional neurite outgrowth was calculated as:

$$Normalized\ directional\ neurite\ density = \frac{Counted\ neurite\ density}{Relative\ myocardium\ volume}$$

RNA sequencing and differential gene expression analysis

Human mesenchymal EPDCs for RNA sequencing were isolated and cultured for 5 days using the same protocol as described above. 4 male and 2 female cryo-preserved mesenchymal EPDCs were isolated and subsequent RNA isolation was performed using the Qiagen mini kit (Qiagen, Hilden, Germany) according to the manufacturers protocol. The final concentration of RNA in each sample was 35 ng/µl. PolyA selection was performed before sequencing. Paired-end sequencing was performed using the Illumina NovaSeq6000 sequencing (Illumina, San Diego, USA) aiming for 20 million paired-end reads per sample. Transcripts were mapped to GRCh37.p13 and Ensemble TranscriptID were annotated using STAR [23]. Quality control was performed using FastQC. A large count table was generated containing raw counts of each transcript. The R package DESeq2 v3.13 was used for differential expression analysis of male versus female EPDCs [24]. A custom design matrix was produced to extract male and female samples only from the count table. Four cryo-preserved male samples were compared to 2 cryo-preserved female samples in the current study. We filtered for >10 total counts per transcript to remove any low count genes. Next, we performed differential gene expression analysis based on negative binomial distribution using the functions provided by the DESeq2 package. Genes were considered differentially expressed if the adjusted p-value was < 0.05.

Pairwise comparisons of cryo-preserved versus non-cryopreserved samples

RNA isolation of human mesenchymal EPDCs was split into two groups: A group in which RNA was isolated from non-cryopreserved EPDCs, and a group in which RNA isolation was performed 5 days after culturing of thawed EPDCs. RNA isolation, sequencing, and quality control was performed as described above. In total, 4 pairs of cryo-preserved and non-cryopreserved samples were used for sequencing.

Next, differential gene expression between cryo-preserved and non-cryopreserved samples were compared per individual sample to exclude inter-individual differences. A custom script was used to analyze the data in a pairwise manner. All raw counts were added by 1 to prevent infinite values in logarithmic fold change values (LogFC). Next, raw counts were annotated with gene name and gene length. This allowed for transformation of raw counts to transcripts per million (TMP). Subsequently, only protein-coding genes with a mean TPM-expression of 5 were included for further analysis. We determined logFC for each pair. Hereafter, 2x2 tables were generated (TPM of gene x + the mean TPM of given sample for 'non-cryo' and 'cryo') and a Fisher Exact test was performed for each gene including multiple testing correction using FDR correction. Gene Ontology pathway enrichment was performed per pair to identify pathways enriched in non-cryopreserved mesenchymal EPDCs compared to cryo-preserved mesenchymal EPDCs using the standard pipeline [25].

Western blotting

Western blotting was performed on both EPDCs supernatant and on cell lysates. Male (n=5) and female (n=4) mesenchymal EPDCs were cultured in a 6-well plate. From confluent cultures the supernatants were collected and samples diluted in Novex Tris-Glycine SDS sample buffer (ThermoFisher, LC2676) and denatured using DTT at 70°C for 10 minutes. After washing in ice cold PBS, EPDCs were lysed with Novex Tris-Glycine SDS sample buffer (ThermoFisher, LC2676) and denatured using DTT at 70°C for 10 minutes. Equal amounts of proteins were size separated using 4-15% Mini-PROTEAN gels (Biorad, 4561084) and transferred to nitrocellulose membranes (Biorad, 1704158) using the Trans-Blot Turbo system of Biorad. Membranes were blocked with 5% milk in TBST and incubated overnight with primary antibody against Slit2 (1:100, Santa Cruz Biotechnology, SC-28945), or Actin (1:1000, Sigma, C6198). After incubation with Horseradish peroxidase (HRP-)conjugated secondary antibodies (1:5000, DAKO) membranes were developed with SuperSignal Western blot Enhancer (ThermoFisher, 46640) and visualized with the ChemiDoc Touch Imaging System (Biorad). Pictures were analyzed using ImageLab software (Biorad) and expression was quantified using ImageJ software from the NIH.

Statistics

Graphs are presented as mean ± SEM. The presence of neurite outgrowth in different conditions was compared using a Chi-square test. Neurites density at different lengths in the M condition and M+EPDCs condition were compared using a paired Student's t-test. Results were considered significant when the p value was < 0.05. GraphPad Prism (GraphPad Software, San Diego, CA, USA; version 9) was used for statistical analysis. RNA sequencing analyses were performed in R version 4.1.1. Scripts are available upon request.

RESULTS

Cryo-preserved EPDCs enhance directional neurite outgrowth towards myocardium

We previously demonstrated enhancing effects of non-cryopreserved human mesenchymal EPDCs on sympathetic neurite outgrowth [17]. For logistic reasons related to limited availability of tissue samples of surgical rest material in past years, we used cryo-preserved EPDCs in the current study. As a first step in our experimental design, we therefore tested whether cryo-preserved EPDCs can also induce directional neurite outgrowth of mouse sympathetic ganglia towards mouse myocardium in co-cultures. While the SCG explants in the control condition showed limited neurite outgrowth, with either absent or short neurites (**Fig. 2A**). The SCG explants cultured in the presence of EPDC (+EPDCs, **Fig. 2B**), myocardium (+M, **Fig. 2C**) or both EPDCs and myocardium (+M+EPDCs, **Fig. 2D**) displayed a clear increase in neurite outgrowth, with regard to both density and length, as compared to the control (SCG only) condition. We also observed strong directional sympathetic neurite outgrowth towards myocardium when culturing SCG in +M and +M+EPDCs conditions (**Fig. 2C, D, E**). Comparison of the occurrence of neurite outgrowth of SCG among the 4 conditions, regardless of the length and density of neurites, confirmed our previous results that EPDCs significantly increase the prevalence of sympathetic directional neurite outgrowth (**Fig. 2E**). For quantification of these results, neurite density was normalized to the myocardial volume in each corresponding co-culture to exclude a potential influence of myocardial volume on neurite outgrowth. The quantification data confirmed that the addition of cryo-preserved EPDCs resulted in a significant increase in directional outgrowth of neurites towards myocardium (**Fig. 2F**), which is in line with our previously published data with non-cryopreserved EPDCs [17].

In contrast to non-cryopreserved EPDCs in our previous experiment [17] , SCG co-cultures with cryo-preserved mesenchymal EPDCs alone showed directional neurite outgrowth towards EPDCs in approximately 30% of co-cultures (**Fig. 2C, F**). RNA sequencing of both groups of EPDCs (cryo-preserved vs. non-cryopreserved) detected several differential expressed genes involved in axonogenesis, such as SEMA4D and PTPRO, which might be related to the neurite

outgrowth differences observed between cryo- and non-cryopreserved EPDCs co-cultures (Supplemental Fig. 1A, B).

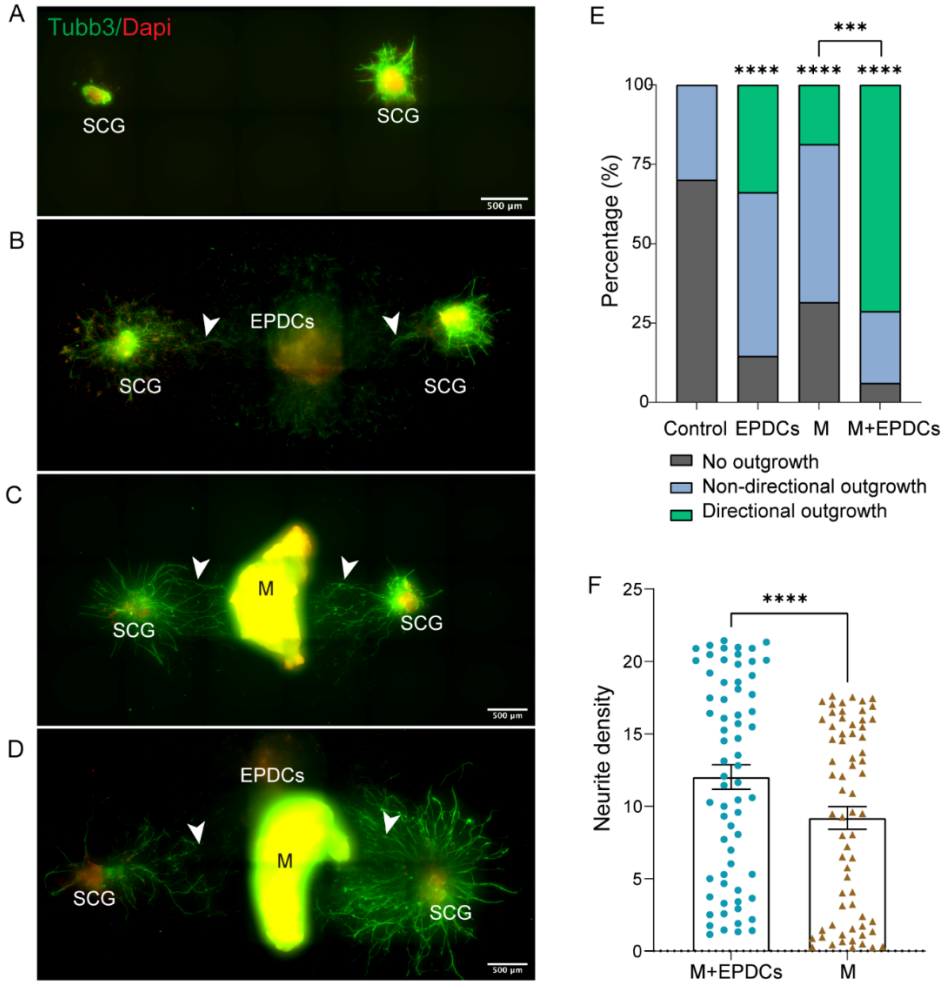

Figure 2. Cryo-preserved EPDCs enhance the directional neurite outgrowth towards myocardium. A-D. Outgrowth of SCG after 6-days of culturing in indicated conditions. A. Control culture of SCG with none or very limited outgrowth. Cryo-preserved EPDCs increase the neurite outgrowth of SCG. Directionally organized neurite outgrowth of SCG towards myocardium are indicated by arrowheads in B, C and D. Scale bar represents 500 µm. E. Quantification of the percentage of SCG showing either no outgrowth (gray), non-directional outgrowth (blue), or directional outgrowth (green). n = 187 for control condition; n = 192 for +EPDCs condition; n = 241 for +M condition; n = 230 for +M+EPDCs condition. Chi-square test was applied to detect the difference among groups, ***P < .001, ****P < .0001 compared to control. F. In +M and +M+EPDCs conditions, when directional outgrowth was detected (green bars in E), the density of directional neurite sprouting towards myocardium was quantified with NeuriteJ. The normalized

density of directional neurites at the length from 50 µm to 1700 µm (interval=25 µm) is shown as a bar plot; each dot represents an average neurite density at each length. n= 48 for +M, n=144 for +M+EPDCs. Paired t-test was applied to detect the difference, ****P < .0001.

Directional neurite outgrowth is significantly higher in male than in female setting

In order to study sex differences in outgrowth of sympathetic neurites, including the enhancing effect of EPDCs on directional neurite outgrowth towards myocardium, we compared co-cultures with an all-female setting and an all-male setting (**Fig. 3A**). In both the female and male settings, co-cultures of ganglia and EPDCs showed that EPDCs significantly increase sympathetic neurite outgrowth (**Fig. 3B, C**). Co-culture with myocardium and EPDCs showed significant promotional effects of the EPDCs on the occurrence of directional neurite outgrowth in both female and male sets (**Fig. 3D, E**).

Quantification of the density of neurites growing directionally towards the myocardium in the absence of EPDCs (+M) or presence of EPDCs (+M+EPDCs) in either a female or male setting, is shown in **Fig. 3F and 3G**. These experiments confirmed that EPDCs significantly enhance directional neurite outgrowth towards myocardium in both female and male settings. However, the directional neurite outgrowth increased by EPDCs seemed more prominent in the male setting (**Fig. 3F, G**). Indeed, comparing male and female neurite density (+M+EPDCs condition) showed a significantly more promotional effect of EPDCs on directional neurite outgrowth in the male compared to the female setting, with on average over the total neurite length a 2 fold increase in males, compared to 1.5 fold increase in females (**Fig. 3H-J**).

Figure. 3 The promotional effects of EPDCs on directional neurite growth is significantly higher in male. A. Schematic representation of the sex information of SCG, EPDCs and myocardium (M) that was utilized in each co-culture group (male and female settings). B-C. Comparison of the percentage of SCG showing neurite outgrowth in the SCG only (control) condition and in the SCG with EPDCs (+EPDCs) condition in the female group and male group. B. Female group, n=78 for control, n=70 for +EPDCs condition. C. Male group, n=77 for control, n=84 for +EPDCs condition. Chi-square test was applied to detect the difference among groups, ****P < .0001. D-E. Comparison of the percentage of SCG showing neurite outgrowth in SCG in the presence of myocardium (+M) or SCG in the presence of myocardium and EPDCs (+M+EPDCs) in female and male groups. D. Results in the female group, n=95 for +M, n=80 for +M+EPDCs. E. Results in the male group, n=87 for +M, n=87 for +M+EPDCs. Chi-square test was applied to detect the difference among groups, ****P < .0001. F-G. In +M and +M+EPDCs conditions, the normalized density of directional neurites at the length from 50 µm to 1700 µm (interval=25 µm) is shown in the bar plot; each dot represents an average neurite density at each length. F. In the female group, n=22 for +M, n=49 for +M+EPDCs. G. In the male group, n=18 for +M, n=59 for +M+EPDC. Paired t-test was applied to detect the difference between +M and +M +EPDCs conditions, **** p < .0001. H-I. Directional neurite density sprouted from SCG cultured in M+EPDCs condition normalized to the averaged directional neurites density of the +M condition in female and male groups. J. Increase of the directional neurite sprouting by EPDCs at the length from 100 µm to 1400 µm (interval=100 µm) is shown in the bar plot. Paired t-test was applied, ** p<0.01. (Figure.3 is on the next page)

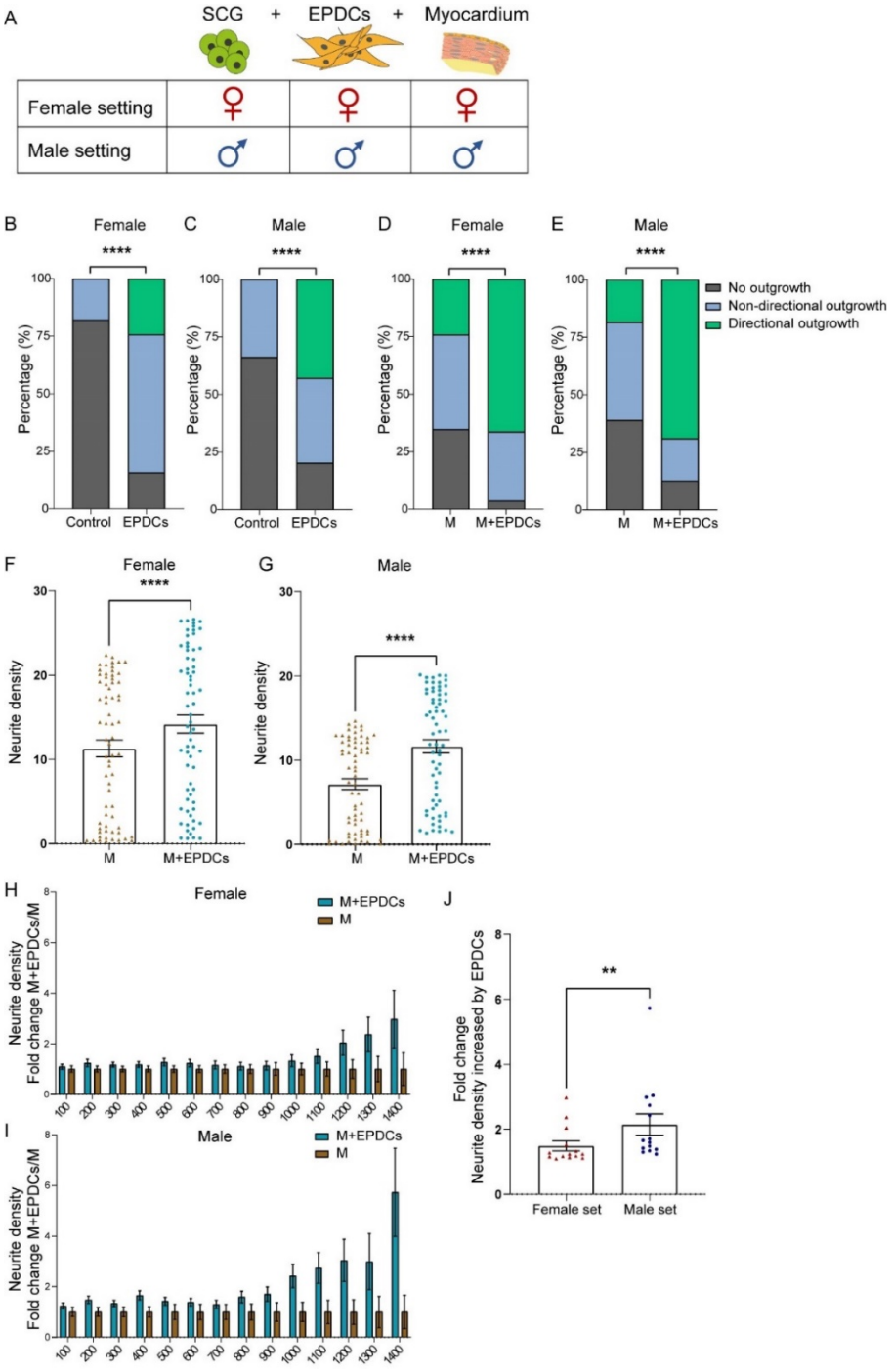
A
SCG + EPDCs + Myocardium
Female setting
Male setting
B Female
C Male
D Female
E Male
****
Percentage (%)
Control EPDCs
M M+EPDCs
No outgrowth
Non-directional outgrowth
Directional outgrowth
F Female
G Male
Neurite density
H Female
I Male
M+EPDCs
M
Neurite density
Fold change M+EPDCs/M
J
Fold change
Neurite density increased by EPDCs
**
Female set
Male set

Male EPDCs in a female setting result in an increased sympathetic neurite growth towards myocardium

As we found a significant larger promotional effect of EPDC on directional neurite outgrowth in the male experimental setting, we hypothesized that male EPDCs would have a similar effect in a female experimental setting. To assess this, we replaced the EPDCs in the female setting with male EPDCs, as illustrated in **Fig. 4A**. Results show that the outgrowth of female sympathetic neurite outgrowth could also be significantly induced by the presence of male EPDCs (**Fig. 4B**), and these male EPDCs in the female setting also displayed significant enhancing effects on the occurrence of directional neurite outgrowth towards myocardium (**Fig. 4C and 4D**), similar to what was seen in the all-male setting. Comparing the neurite density between male and female EPDCs in a female setting, we observed a higher sympathetic neurite outgrowth towards myocardium in the presence of male EPDCs (**Fig. 4E and 4F**). Moreover, comparing this co-culture containing male EPDCs in a female setting with an all-male setting showed no difference in the neurite density of the directional sympathetic outgrowth towards myocardium induced by male EPDCs (**Fig. 4G and 4H**). Collectively, these data demonstrate that the enhancing effect of male EPDCs in a female setting on sympathetic neurite growth towards myocardium, is not due to a lack of neurite outgrowth capacity of the female SCG, but rather due to a less robust promotional effect of female EPDCs as compared to male EPDCs on neurite outgrowth.

Figure. 4 Male EPDCs in a female setting highly promote sympathetic neurite growth towards myocardium. A. Schematic representation of the sex information of SCG, EPDCs and myocardium (M) that was used in each co-culture group (male or female EPDCs in female setting). B. Comparison of the percentage of SCG showing neurite outgrowth in the control condition and in the EPDC condition in the male EPDCs (in a female setting) group. n=19 for control, n=23 for +EPDCs condition. C. Comparison of the percentage of SCG showing neurite outgrowth in the presence of myocardium (+M) or SCG in the presence of myocardium and male EPDCs (+M+EPDCs) in the female setting. n=35 for +M, n=35 for +M+EPDCs. Chi-square test was applied to detect the difference among groups, ****P < .0001. D. In +M and +M+EPDCs conditions of male EPDCs group (in a female setting), the normalized density of directional neurites at the length from 50 µm to 1400 µm (interval=100 µm) is shown in the bar plot; each dot represents an average neurite density at each length. n= 4 for +M, n= 20 for +M+EPDC. Paired t-test was applied to detect the difference between +M and +M +EPDCs conditions, **** p < .0001. E. Directional neurite density sprouted from SCG cultured in M+EPDCs condition normalized to the averaged directional neurites density of the +M condition in male EPDCs group. F. The increase of the directional neurite sprouting by male EPDCs at the length from 100 µm to 1400 µm (interval=100 µm) is shown. Paired t-test was applied, * p<0.05. G-H. Comparison of male EPDCs in the female setting, with the male setting. ns, no significant difference. **(Figure.4 is on the next page)**

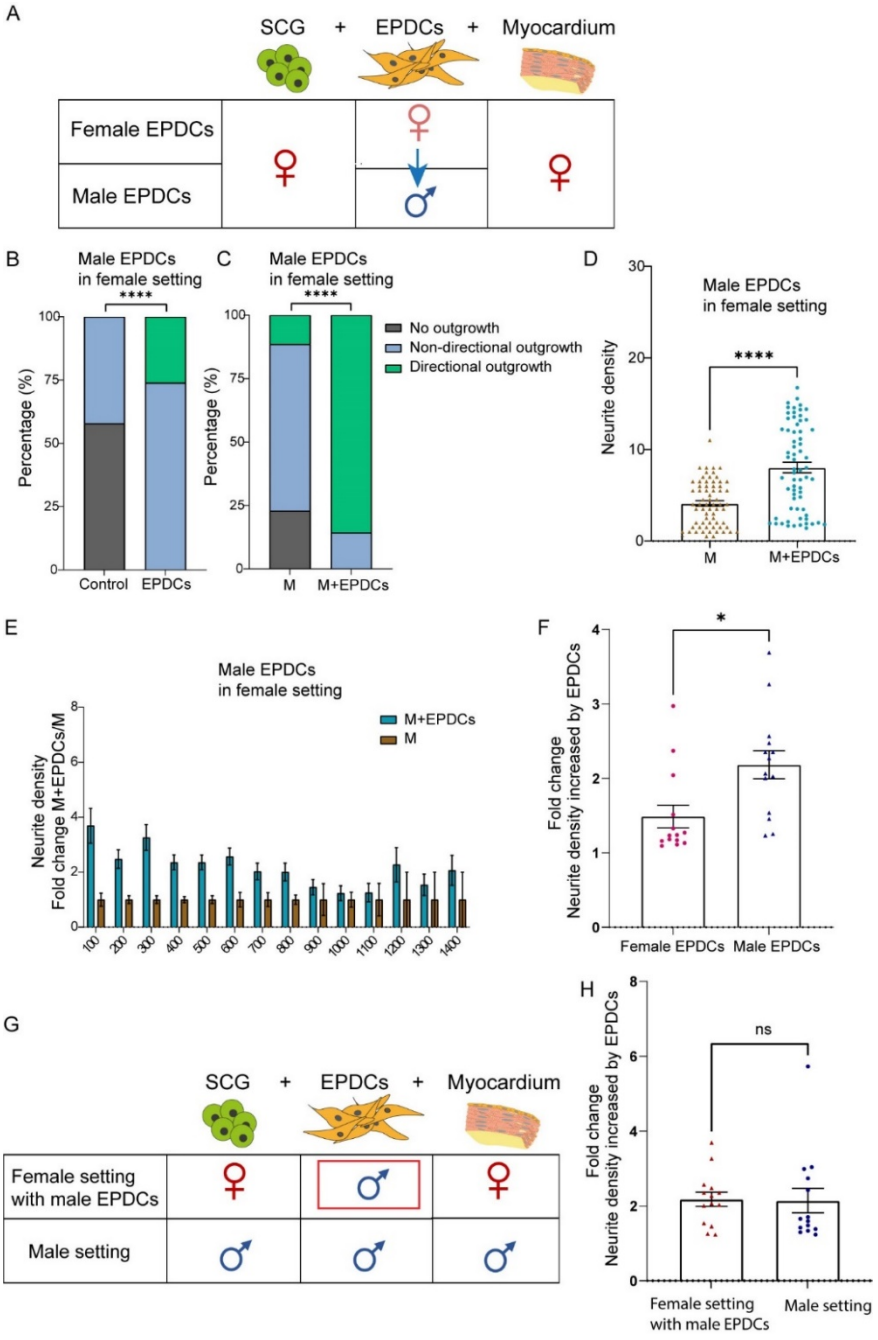
A
SCG + EPDCs + Myocardium
Female EPDCs
Male EPDCs
B
Male EPDCs in female setting
****
Percentage (%)
Control
EPDCs
C
Male EPDCs in female setting
****
No outgrowth
Non-directional outgrowth
Directional outgrowth
M
M+EPDCs
D
Male EPDCs in female setting
****
Neurite density
M
M+EPDCs
E
Male EPDCs in female setting
M+EPDCs
M
Neurite density
Fold change M+EPDCs/M
F
*
Fold change
Neurite density increased by EPDCs
Female EPDCs
Male EPDCs
G
SCG + EPDCs + Myocardium
Female setting with male EPDCs
Male setting
H
ns
Fold change
Neurite density increased by EPDCs
Female setting with male EPDCs
Male setting

Differential expression of SLIT2 between male and female EPDCs

As we found a more robust capacity of male EPDCs to stimulate neurite outgrowth in comparison to female EPDCs, we next assessed the difference in gene expression between male and female EPDC by RNA sequencing and differential gene expression analysis. This revealed differentially higher and lower expressed genes in males compared to female EPDCs (**Supplemental Table 1**), which might contribute to the sex difference of EPDCs in promoting directional neurite growth. One of the genes showing a differential expression was SLIT2, that is known to regulate axon growth during central nervous system development [26, 27]. Immunoblot analysis confirmed that female EPDCs had more cell-associated SLIT2 protein (**Fig. 5**), which was paralleled by more SLIT2 in cell culture supernatants of female EPDCs compared to cell culture supernatants of male EPDCs (**Fig. 5**).

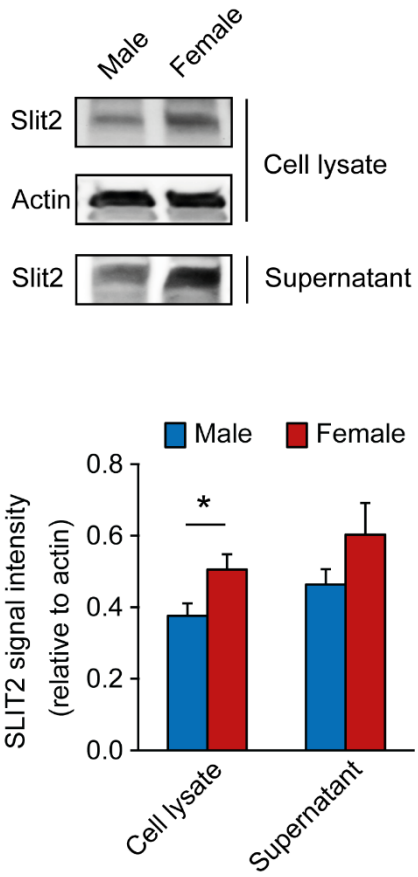

Figure. 5 Western blotting of SLIT2 in male and female EPDCs. Western blot images and analysis of SLIT2 expression in male (n=5) and female (n=4) mesenchymal EPDCs and secreted SLIT2 in corresponding culturing supernatant. * P<0.05.

DISCUSSION

The influence of sex in the prevalence and outcomes of cardiovascular disease has increasingly been recognized over the past decades. In line with this, a growing number of researchers acknowledges the relevance of taking sex into account in both clinical and basic science. We have previously shown a stimulating role of mesenchymal EPDCs on outgrowth of SCG in vitro [17], but did not take sex of the cell donor into account yet. In the present study we performed co-cultures of sympathetic ganglia with myocardium and mesenchymal EPDCs to specifically study the effect of the sex of EPDCs on cardiac innervation. Key findings of our study are: i) Cryo-preserved EPDCs promote sympathetic neurite outgrowth *in vitro* and increase the directional neurite projection towards myocardium; ii) In the presence of EPDCs, male SCG exhibit higher cardiac sympathetic outgrowth than female SCG; iii) Male EPDCs in a female setting can increase the cardiac sympathetic neurite outgrowth to a level that is comparable to the level of outgrowth in an entirely male environment; And iv) The SLIT2/ROBO-pathway is proposed as a potential candidate influencing these differential findings in male and female EPDCs.

Findings of the current study have potential clinical implications. There are overt sex-differences in the occurrence of clinical arrhythmias, with a general higher tendency of ventricular tachycardia and sudden cardiac death to occur in males [28]. In addition, sex differences in autonomic function, of relevance for a.o. cardiac repolarization, have been shown [29, 30]. This is of interest in the light of the phenomenon of sympathetic hyperinnervation, that is increasingly recognized as a mechanism of ventricular tachycardia and sudden cardiac death in structural heart disease [31, 32].

Cardiac autonomic ganglia and nerve fibers have their developmental origin in the neural crest, multipotent cells that derive from the crest of the embryonic neural plate [33, 34]. Already in utero, sex differences in autonomic cardiac function have been observed [35]. Ventricular autonomic innervation develops in parallel with ventricular vascularization, guided by neurotrophic factors [36]. We have previously shown a pivotal role of the epicardium in the development of the cardiac autonomic nerve system [37], a study that initiated the concept of a potential role of the epicardium in cardiac autonomic innervation. Whereas in the healthy adult heart the epicardium is considered as a quiescent layer, which can become activated in response to pathological triggers, such as MI [38]. In mouse models, experimentally-induced MI re-activates the epicardium, both endogenous and transplanted exogenous human EPDCs migrate to the infarcted area and contribute to neovascularization and amelioration of LV function [38-41]. In many of the these animal studies, sex has not been not taken into account. As MI is still the number one cause of death in the western countries, not only in men, but at higher age, after menopause, also in women [42], this is certainly a subject that deserves

attention, as is increasingly recognized [43]. Reperfusion therapy after MI has significantly reduced mortality and morbidity, but there is still a high risk of early ventricular arrhythmias and mortality. Next to the mechanism of re-entry in the border zone [44], this has in the past decades increasingly been associated with sympathetic hyperinnervation, also an early event after MI, starting within a few hours to several weeks after the ischemic event. Sympathetic hyperinnervation, defined as a superfluous increase of sympathetic fibers in the heart after MI, has been linked to sympathetic overactivity with a risk of ventricular arrhythmias [45-47]. Although data is still scarce, several studies have indicated that post-MI arrhythmias induced by sympathetic hyperinnervation are more severe in males than in females [6, 48]. Although our experiments were performed in an *in-vitro* non-MI setting, results of our co-cultures of sympathetic autonomous ganglia with ventricular myocardium and activated EPDCs, are in line with these clinical observations, showing a higher directional sympathetic neurite projection towards the myocardium in male than in female.

In addition to the evaluation of sex differences in sex-matched conditions (the so-called female setting and male setting), we aimed to study whether the observed difference in outgrowth between male and female tissues was attributable to a diminished capacity of female ganglia to grow, or whether this was caused by the "female" environment. We therefore tested the hypothesis that female ganglia would show a similar growth capacity as male ganglia, in the presence of male EPDCs. Results showed that co-culturing male EPDCs in a female environment (i.e. with female myocardium and female SCG) causes an increase in cardiac sympathetic neurite outgrowth to a level that is comparable to the level of outgrowth in an entirely male environment. In line with this, we observed a lower expression of SLIT2 in male EPDCs as compared to female EPDCs. SLIT2 is a member of a family of large extracellular matrix (ECM) glycoproteins and has been described as a chemorepellent factor for axonogenesis in motor neurons [49-52]. Inhibition studies of the SLIT2/ROBO signaling pathway will be necessary to determine its exact role in epicardial stimulation of cardiac innervation and the role of sex therein.

Cryo-preserved versus non-cryopreserved EPDCs. For quantification of our results, we have used so called "directional outgrowth" as parameter, defined as the outgrowth in the quadrant bordering the target tissue, i.e. the myocardium. In our previous study, using non-cryopreserved EPDCs, we did not observe directional outgrowth towards EPDCs, but only towards the myocardium [17]. Of interest, in our current study design, we used cryopreserved EPDCs, due to a lack of sufficient supply of fresh EPDCs in the past years, partly attributable to the downscaling of surgical procedures during the Covid19 pandemic. As expected, both cryo-preserved EPDCs and non-cryopreserved EPDCs could promote sympathetic neurite outgrowth. However, in contrast to our previous study, we observed that cryo-preserved

EPDCs could also attract neurite projections, i.e. directional outgrowth was observed in the EPDC-SCG cultures, in the absence of myocardium. As these findings might indicate a differential expression of axonal guidance and attraction related factors in cryo-preserved versus non-cryopreserved EPDCs, we performed RNA seq of both types (i.e. cryo- versus non-cryopreserved EPDCs). RNA sequencing and DGE analysis of 4 pairs of cryo-preserved EPDCs versus non-cryopreserved EPDCs indeed indicated differentially expressed axonogenesis related genes, including SEMA4D, PTPRO. PTPRO (protein tyrosine phosphatase receptor type O), is known to support axonogenesis of the nervous system as well as NGF-dependent neuronal outgrowth [53, 54], and this transmembrane receptor is required in growing neurons. The role of PTPRO in EPDCs is currently unknown. SEMA4D, as a member of Semaphorin family of soluble and transmembrane proteins, participates in multiple key cellular functions including axon guidance and morphogenesis [55]. Although not the focus of our current study, further research is needed to evaluate potential effects of cryo-preservation on neurotrophic function of EPDCs.

Conclusions, clinical implications and future perspectives

In summary, in the current study, we show a stimulatory effect of cryopreserved EPDCs on neurite outgrowth *in vitro*. Our co-cultures in female and male settings demonstrate that sympathetic nerve outgrowth and density differs between male and female, with a higher stimulatory effect of male - as compared to female - EPDCs. This differential effect could be neutralized by changing the sex of the EPDCs. We propose the SLIT2/ROBO pathway as a potential candidate involved in these sex-differences observed.

Although our results are preliminary and require validation in broader experimental settings, our data underline the potential relevance of sex differences in post-MI arrhythmias related cardiac hyperinnervation. In addition, results indicate that the sex of the individuals that EPDCs are derived from can influence the response significantly with respect to the amount of outgrowth and neurite density. Considering the current focus on cell therapy, including induced pluripotent stem cells, cardiomyocyte progenitor cells and EPDCs, in preserving heart function after cardiac damage [56, 57], we propose that sex should be taken into account when considering injection of cells for cell therapy in male and female patients.

Future directions. In the present study we focused on the influence of the sex of EPDCs in cardiac sympathetic innervation in vitro, using 3D co-cultures with sympathetic ganglia, myocardium and EPDCs. As a next step, we aim to further validate our results by performing SLIT2 knock down and overexpression in male and female EPDCs and evaluate the presence of the receptors of Slit2 (ROBO receptors) on cardiac sympathetic autonomous ganglia. In addition, the role of hormones deserve more attention. Whether these sex differences are

detectable in cardiac sympathetic activity *in vivo* or affect prognosis of patients suffering MI also requires further study and validation.

AUTHOR CONTRIBUTIONS

All authors contributed to the study conception and design. The experiments were designed and performed by Y.G. and J.M.v.G., analyzed by Y.G and supervised by M.R.M.J. and M.C.d.R. RNA-seq analysis was perform by R.M and Y.G. The first draft of the manuscript was written by Y.G., J.M.v.G., M.R.M.J., M.C.d.R. All authors commented on the manuscript. All authors have read and agreed to the published version of the manuscript.

FUNDING

This work is supported by the Netherlands Organization for Scientific Research (NWO) [016.196.346 to M.R.M.J] and in part by European Research Area Network on Cardiovascular Diseases and Dutch Heart Foundation [038 MISsCVD 2018T095 to J.M.v.G.] and ZonMW [84920 Size Matters to M.C.d.R].

ACKNOWLEDGMENTS

We are grateful to Tessa van Herwaarden (Department of Cell and Chemical Biology, LUMC, Leiden, The Netherlands) for her help with isolating primary human EPDCs.

CONFLICTS OF INTEREST

The authors declare no conflict of interest.

REFERENCES

1. Zipes, D.P. and H.J. Wellens, *Sudden cardiac death.* Circulation, 1998. 98(21): p. 2334-51.
2. Myerburg, R.J. and M.J. Junttila, *Sudden cardiac death caused by coronary heart disease.* Circulation, 2012. 125(8): p. 1043-52.
3. Davis, E., et al., *"Mind the gap" acute coronary syndrome in women: A contemporary review of current clinical evidence.* International Journal of Cardiology, 2017. 227: p. 840-849.
4. EUGenMed, T., et al., *Gender in cardiovascular diseases: impact on clinical manifestations, management, and outcomes.* European Heart Journal, 2015. 37(1): p. 24-34.
5. Burger, I.A., et al., *Age- and sex-dependent changes in sympathetic activity of the left ventricular apex assessed by 18F-DOPA PET imaging.* PLoS One, 2018. 13(8): p. e0202302.
6. Dart, A.M., X.-J. Du, and B.A. Kingwell, *Gender, sex hormones and autonomic nervous control of the cardiovascular system.* Cardiovascular Research, 2002. 53(3): p. 678-687.
7. Smetana, P. and M. Malik, *Sex differences in cardiac autonomic regulation and in repolarisation electrocardiography.* Pflügers Archiv - European Journal of Physiology, 2013. 465(5): p. 699-717.
8. Regitz-Zagrosek, V., et al., *Gender in cardiovascular diseases: impact on clinical manifestations, management, and outcomes.* Eur Heart J, 2016. 37(1): p. 24-34.
9. Curtis, A.B. and D. Narasimha, *Arrhythmias in women.* Clin Cardiol, 2012. 35(3): p. 166-71.
10. Kannel, W.B., et al., *Sudden coronary death in women.* Am Heart J, 1998. 136(2): p. 205-12.
11. Wittnich, C., et al., *Sex differences in myocardial metabolism and cardiac function: an emerging concept.* Pflügers Archiv - European Journal of Physiology, 2013. 465(5): p. 719-729.
12. Ajijola, O.A., et al., *Extracardiac Neural Remodeling in Humans With Cardiomyopathy.* 2012. 5(5): p. 1010-1116.
13. Nguyen, B.L., et al., *Acute myocardial infarction induces bilateral stellate ganglia neural remodeling in rabbits.* Cardiovasc Pathol, 2012. 21(3): p. 143-8.
14. Ajijola, O.A., et al., *Remodeling of stellate ganglion neurons after spatially targeted myocardial infarction: Neuropeptide and morphologic changes.* Heart Rhythm, 2015. 12(5): p. 1027-35.
15. Bayles, R.G., et al., *Transcriptomic and neurochemical analysis of the stellate ganglia in mice highlights sex differences.* Sci Rep, 2018. 8(1): p. 8963.
16. Bayles, R.G., et al., *Sex differences in sympathetic gene expression and cardiac neurochemistry in Wistar Kyoto rats.* PLoS One, 2019. 14(6): p. e0218133.
17. Ge, Y., et al., *Human epicardium-derived cells reinforce cardiac sympathetic innervation.* J Mol Cell Cardiol, 2020. 143: p. 26-37.
18. Cao, J. and K.D. Poss, *The epicardium as a hub for heart regeneration.* Nature reviews. Cardiology, 2018. 15(10): p. 631-647.
19. Smits, A.M., E. Dronkers, and M.-J. Goumans, *The epicardium as a source of multipotent adult cardiac progenitor cells: Their origin, role and fate.* Pharmacological Research, 2018. 127: p. 129-140.
20. Quijada, P., M.A. Trembley, and E.M. Small, *The Role of the Epicardium During Heart Development and Repair.* Circulation Research, 2020. 126(3): p. 377-394.
21. Dronkers, E., et al., *The Isolation and Culture of Primary Epicardial Cells Derived from Human Adult and Fetal Heart Specimens.* J Vis Exp, 2018(134).
22. Torres-Espín, A., et al., *Neurite-J: an image-J plug-in for axonal growth analysis in organotypic cultures.* J Neurosci Methods, 2014. 236: p. 26-39.
23. Dobin, A., et al., *STAR: ultrafast universal RNA-seq aligner.* Bioinformatics, 2013. 29(1): p. 15-21.

24. Love, M.I., W. Huber, and S. Anders, *Moderated estimation of fold change and dispersion for RNA-seq data with DESeq2.* Genome Biol, 2014. 15(12): p. 550.
25. Mi, H., et al., *PANTHER version 14: more genomes, a new PANTHER GO-slim and improvements in enrichment analysis tools.* Nucleic Acids Res, 2019. 47(D1): p. D419-d426.
26. Lin, L., Y. Rao, and O. Isacson, *Netrin-1 and slit-2 regulate and direct neurite growth of ventral midbrain dopaminergic neurons.* Mol Cell Neurosci, 2005. 28(3): p. 547-55.
27. Battisti, A.C., et al., *A subset of chicken statoacoustic ganglion neurites are repelled by Slit1 and Slit2.* Hear Res, 2014. 310: p. 1-12.
28. Ehdaie, A., et al., *Sex Differences in Cardiac Arrhythmias: Clinical and Research Implications.* Circ Arrhythm Electrophysiol, 2018. 11(3): p. e005680.
29. Dart, A.M., X.J. Du, and B.A. Kingwell, *Gender, sex hormones and autonomic nervous control of the cardiovascular system.* Cardiovasc Res, 2002. 53(3): p. 678-87.
30. Smetana, P. and M. Malik, *Sex differences in cardiac autonomic regulation and in repolarisation electrocardiography.* Pflugers Arch, 2013. 465(5): p. 699-717.
31. Nederend, I., et al., *Postnatal Cardiac Autonomic Nervous Control in Pediatric Congenital Heart Disease.* Journal of cardiovascular development and disease, 2016. 3(2): p. 16.
32. Zipes, D.P. and M. Rubart, *Neural modulation of cardiac arrhythmias and sudden cardiac death.* Heart rhythm, 2006. 3(1): p. 108-113.
33. Lumb, R. and Q. Schwarz, *Sympathoadrenal neural crest cells: the known, unknown and forgotten?* Dev Growth Differ, 2015. 57(2): p. 146-57.
34. Végh, A.M.D., et al., *Part and Parcel of the Cardiac Autonomic Nerve System: Unravelling Its Cellular Building Blocks during Development.* J Cardiovasc Dev Dis, 2016. 3(3).
35. Gonçalves, H., et al., *Gender-specific evolution of fetal heart rate variability throughout gestation: A study of 8823 cases.* Early Hum Dev, 2017. 115: p. 38-45.
36. Nam, J., et al., *Coronary veins determine the pattern of sympathetic innervation in the developing heart.* Development, 2013. 140(7): p. 1475-85.
37. Kelder, T.P., et al., *The epicardium as modulator of the cardiac autonomic response during early development.* J Mol Cell Cardiol, 2015. 89(Pt B): p. 251-9.
38. Winter, E.M., et al., *Preservation of left ventricular function and attenuation of remodeling after transplantation of human epicardium-derived cells into the infarcted mouse heart.* Circulation, 2007. 116(8): p. 917-27.
39. Smart, N., K.N. Dubé, and P.R. Riley, *Epicardial progenitor cells in cardiac regeneration and neovascularisation.* Vascul Pharmacol, 2013. 58(3): p. 164-73.
40. Limana, F., M.C. Capogrossi, and A. Germani, *The epicardium in cardiac repair: from the stem cell view.* Pharmacol Ther, 2011. 129(1): p. 82-96.
41. van Wijk, B., et al., *Cardiac regeneration from activated epicardium.* PLoS One, 2012. 7(9): p. e44692.
42. WHO. *The top 10 causes of death*. 2020; Available from: https://www.who.int/news-room/fact-sheets/detail/the-top-10-causes-of-death.
43. Korzick, D.H. and T.S. Lancaster, *Age-related differences in cardiac ischemia-reperfusion injury: effects of estrogen deficiency.* Pflugers Arch, 2013. 465(5): p. 669-85.
44. de Bakker, J.M., et al., *Slow conduction in the infarcted human heart. 'Zigzag' course of activation.* Circulation, 1993. 88(3): p. 915-26.
45. Zhou, S., et al., *Mechanisms of Cardiac Nerve Sprouting After Myocardial Infarction in Dogs.* Circulation Research, 2004. 95(1): p. 76-83.
46. Chen, P.-S., et al., *Sympathetic nerve sprouting, electrical remodeling and the mechanisms of sudden cardiac death.* Cardiovascular Research, 2001. 50(2): p. 409-416.

47. Yokoyama, T., et al., *Quantification of sympathetic hyperinnervation and denervation after myocardial infarction by three-dimensional assessment of the cardiac sympathetic network in cleared transparent murine hearts.* PLoS One, 2017. 12(7): p. e0182072.
48. Du, X.J., et al., *Sympathetic activation triggers ventricular arrhythmias in rat heart with chronic infarction and failure.* Cardiovasc Res, 1999. 43(4): p. 919-29.
49. Ba-Charvet, K.T.N., et al., *Slit2-Mediated Chemorepulsion and Collapse of Developing Forebrain Axons.* Neuron, 1999. 22(3): p. 463-473.
50. Niclou, S.P., L. Jia, and J.A. Raper, *Slit2 is a repellent for retinal ganglion cell axons.* The Journal of neuroscience : the official journal of the Society for Neuroscience, 2000. 20(13): p. 4962-4974.
51. Tanno, T., et al., *Expression of a chemorepellent factor, Slit2, in peripheral nerve regeneration.* Biosci Biotechnol Biochem, 2005. 69(12): p. 2431-4.
52. Li, Y., et al., *Slit2/Robo1 promotes synaptogenesis and functional recovery of spinal cord injury.* Neuroreport, 2017. 28(2): p. 75-81.
53. Beltran, P.J., J.L. Bixby, and B.A. Masters, *Expression of PTPRO during mouse development suggests involvement in axonogenesis and differentiation of NT-3 and NGF-dependent neurons.* J Comp Neurol, 2003. 456(4): p. 384-95.
54. Chen, B. and J.L. Bixby, *A novel substrate of receptor tyrosine phosphatase PTPRO is required for nerve growth factor-induced process outgrowth.* J Neurosci, 2005. 25(4): p. 880-8.
55. Koncina, E., et al., *Role of semaphorins during axon growth and guidance.* Adv Exp Med Biol, 2007. 621: p. 50-64.
56. Abdelwahid, E., et al., *Stem cell therapy in heart diseases: a review of selected new perspectives, practical considerations and clinical applications.* Curr Cardiol Rev, 2011. 7(3): p. 201-12.
57. Hashimoto, H., E.N. Olson, and R. Bassel-Duby, *Therapeutic approaches for cardiac regeneration and repair.* Nature Reviews Cardiology, 2018. 15(10): p. 585-600.

SUPPLEMENTAL FIGURES

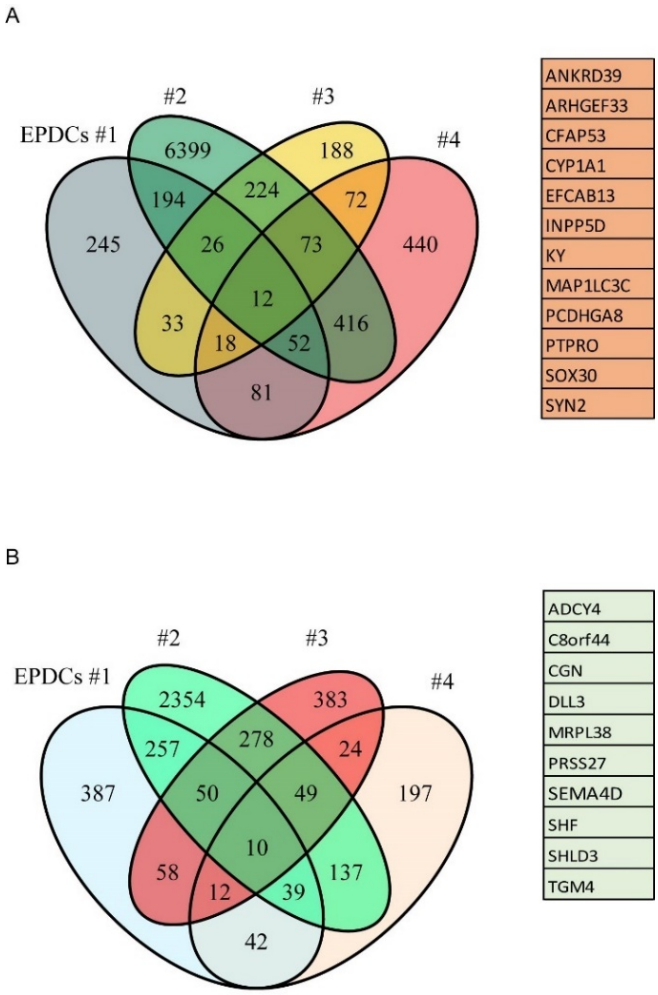

Supplemental Fig. 1 Differential gene expression analysis between cryo-preserved versus non-cryopreserved EPDCs. A. Venn diagram of 4 donate-derived EPDCs (EPDCS#1, #2, #3, #4) shows 12 common protein-coding genes that up-regulated in cryo-preserved EPDCs compared to non-cryo-preserved EPDCs. B. Venn diagram of 4 donor-derived EPDCs (EPDCS#1, #2, #3, #4) shows the 10 common protein-coding genes down-regulated in cryo-preserved EPDCs compared to non-cryo-preserved EPDCs. The detected up- and down-regulated genes are listed in the right panels.

Genes	adjusted P value	LogFC
ERVV-1	5,68E-05	24,02632
UPK3B	4,12E-02	6,216895
LRRN4	6,74E-03	5,726742
HTT	9,73E-03	4,135993
KRT19	2,31E-02	3,035461
ITGA7	1,70E-02	2,529226
SLIT2	4,84E-02	1,134702
PKD1P5	2,35E-02	-3,29221
ID1	2,40E-03	-3,49841
EIF1AY	6,59E-03	-7,8285
NLGN4Y	6,59E-03	-7,87928
TXLNGY	6,04E-03	-7,92583
KDM5D	2,03E-03	-8,43109
ZFY	2,03E-03	-8,45093
RPS4Y1	2,03E-03	-8,47819
USP9Y	1,28E-03	-8,84273

Supplemental Table. 1 DGE analysis of male EPDCs between female EPDCs. Highly differentially expressed genes in male EPDCs as compared to female EPDCs are shown in the table. Green highlights indicate the genes are lower expressed in male EPDCs while the red indicate the higher expressed gene in male than in female.